

## SECONDARY-ELECTRON EMISSION FROM HYDROGEN-TERMINATED DIAMOND

Erdong Wang<sup>#</sup>, Ilan Ben-Zvi, Triveni Rao, Qiong Wu, Brookhaven National Laboratory, Upton, NY 11973, USA

D.A.Dimitrov Tech-X Corp., Boulder, CO 80303, USA

Tianmu Xin Physics and Astronomy Department, Stony Brook University, Stony Brook, NY 11974, USA

### Abstract

Diamond amplifiers demonstrably are an electron source with the potential to support high-brightness, high-average-current emission into a vacuum. We recently developed a reliable hydrogenation procedure for the diamond amplifier. The systematic study of hydrogenation resulted in the reproducible fabrication of high gain diamond amplifier. Furthermore, we measured the emission probability of diamond amplifier as a function of the external field and modelled the process with resulting changes in the vacuum level due to the Schottky effect. We demonstrated that the decrease in the secondary electrons' average emission gain was a function of the pulse width and related this to the trapping of electrons by the effective NEA surface. The findings from the model agree well with our experimental measurements. As an application of the model, the energy spread of secondary electrons inside the diamond was estimated from the measured emission.

### INTRODUCTION

Assuring a high-brightness, high average current and low emittance electron beam is required by new light source based on energy recovery linac. The diamond demonstrably is a stable electron source that potentially meets the request of energy recovery linac.

The diamond, functioning as a secondary emitter, amplifies the primary current[1]. Primary electrons with energy of a few keV penetrate the diamond through the metal coating, and excite electron-hole pairs. A fraction of secondary electrons drift across the diamond under the electric field and reach the hydrogen-terminated surface. Except the electrons are emitted, the rest are trapped and accumulate on the surface until the external electric field is shielded totally. Therefore, the field inside the diamond, transmitted charge and emitted charge are time dependent. The probability of the emission of an electron that arrives at the emission surface is depending on diamond surface condition, hydrogenation quality and external field. In this article, we describe our optimization of the hydrogenation process which results in high quality diamond amplifiers being reproducible. To understand the

mechanism for electrons trapping and its external conditions dependent, we measured the emission probability of four diamond amplifiers as a function of the external field and modelled the process with the resulting changes in the vacuum level due to the Schottky effect.

### HYDROGENATION OPTIMIZATION

We carried out the hydrogenation experiments in a UHV chamber. Our set-up for hydrogenation, details is published elsewhere[2]. To fabricate a diamond amplifier, we Pt-coated one side of high purity 4\*4mm<sup>2</sup>, 300um-thick single-crystal diamond samples, grown by chemical deposition (CVD); the other side was hydrogenated.

We compared four diamonds hydrogenated at room temperature with four others treated at high temperatures. For the latter, after temperature of the diamond reached 800 °C, the heater was turned off; hydrogenation was started, and continued as the sample's temperature decreased gradually to 320°C. For room-temperature hydrogenation, the sample was allowed to cool down to 23°C before starting hydrogenation. For both the hydrogen partial pressure was 1.3\*10<sup>-6</sup>hPa. Figure 1 shows a typical curve for photocurrent yield from the hydrogenated surface of sample treated at 800°C (dark curve) and at 23°C (gray curve).

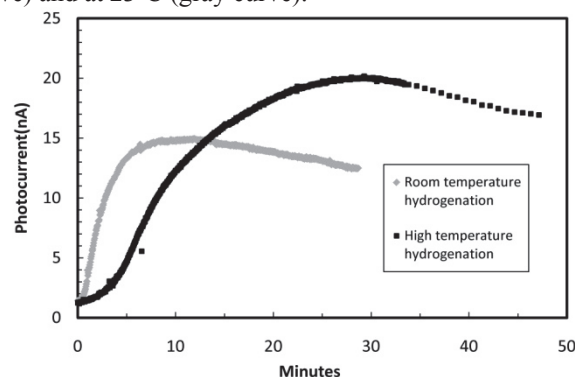


Figure 1: The trend in the photocurrent during the hydrogenation process. Dark curve represents the trend during high-temperature hydrogenation, and the gray curve is that at room temperature.

As Figure 1 shows, the photocurrent took 30 minutes to reach a peak when the diamond was hydrogenated at high temperature; in contrast, during hydrogenation at 23°C, the photocurrent peaked in 10 minutes. The speed of

\*Work supported by Brookhaven Science Associates, LLC under Contract No. DE-AC02-98CH10886 and at Stony Brook University under grant DE-SC0005713 with the U.S. DOE.

<sup>#</sup>wange@bnl.gov

hydrogen deposition differed at these two different temperatures. At high temperatures, hydrogen attaches to and detaches from the carbon atoms. Hence, it takes longer to reach optimum coverage than when the process is carried out at room temperature at which the detachment of hydrogen is insignificant. Further hydrogenation does not increase the coverage. However, it exposes the sample to contaminants released from the cracker that may cause impinge on the diamond's NEA surface causing the photo current to decay. This reduction was unrecoverable by subsequent re-baking or re-hydrogenation. Figure 2 shows the photocurrent decays of the high-temperature and room-temperature hydrogenation process. At the end of hydrogenation (after the cracker was turned off and the hydrogen pumped from the system), the change in photocurrent over time was measured with 220 nm beam. In 11 hours, the photocurrent of the diamond processed at high temperature dropped 13%, while that of the diamond treated at room temperature declined 50%; thus, the NEA surface produced via high-temperature hydrogenation is more stable than that created at room temperature. The decay curve of the room temperature hydrogenation has two components, one with a decay time of 0.25 hours, and a slow component where the decay time (~4.76 hours) is common to both processes curves. Such loss of photocurrent can be recovered by baking the sample. Thus, after the decay of the photocurrent in 11 hours, we baked the diamonds at 400°C for 30 minutes. There was almost full recovery (99%) of the photocurrent of the diamond that underwent high-temperature hydrogenation; the decay of the photocurrent under this condition is due to contaminants, such as water absorbed on the hydrogenated surface that are desorbed to the surface during baking [3]. However, the photocurrent of the diamond hydrogenated at the room temperature exhibited only 65% recovery after baking, implying that baking can correct the slow decay, but not that lost during the fast decay.

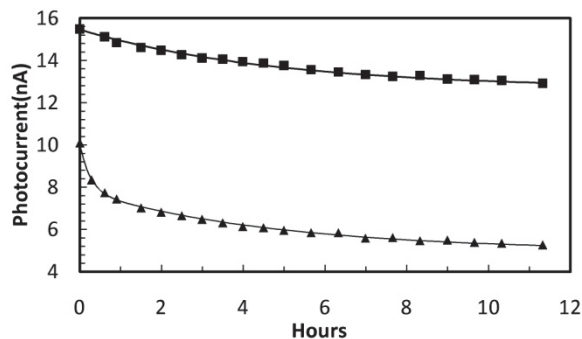


Figure 2: The stabilization of the photocurrent of hydrogenated diamonds in 11 hours. The solid square is the photocurrent of the high-temperature-treated diamond; the solid triangle is the photocurrent of hydrogenation decay at room temperature. The thin black curves are the best fit functions.

The diamond amplifier is extremely robust and is stable during exposure to air; the water vapor in the air inhibits electron emission from it[3]. Heating diamonds exposed

to the atmosphere removes water molecules from their surfaces. We explored the optimal temperature for such evaporation; the photocurrent of the diamond amplifier with a new hydrogenation surface is 17nA. After exposure to air for 1 hour, the emission current falls to 2nA. We then heated the diamond to the 200° C for 30 minutes and left it to cool. Our measurements of the photocurrent shows the diamond's photocurrent rebounded to 10nA. We scanned the photocurrent as a function of the temperature of the heat treatment and found the optimized temperature for heat treatment is 450°C after which the photocurrent recovered to 96% of that of an amplifier unexposed to the atmosphere. The findings prove that the quality of hydrogenation is recovered by baking. Temperatures higher than 450°C break the hydrogen- and carbon-bonds. At 800°C, hydrogen atoms are removed from the diamond surfaces, leaving it bare.

## GAIN MEASUREMENT

We start by defining various variables (Figure 3), wherein  $I_p$  is the DC primary current, and the generated average secondary electron current is  $I_s$ . The instantaneous secondary electrons current reaching the emission surface is  $I_i(t)$ . The instantaneous current emitted from the diamond is defined as  $I_e(t)$ . The measured average emission secondary- electron current is

$$I_a = \frac{\int_0^w I_e(t) dt}{1/f}$$

where  $f$  is the pulse repetition frequency and  $w$  is the high voltage pulse width. The instantaneous

transmission gain is defined as  $G_t = \frac{I_i}{I_p}$ . We further

$$\text{define the average emission gain as } G_e = \frac{I_a}{I_p} \frac{1}{f \cdot w}$$

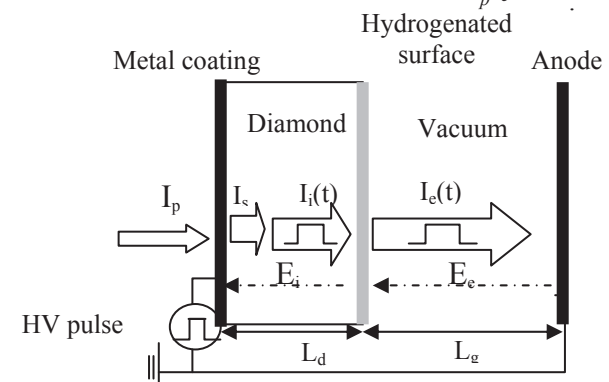


Figure 3: The definitions of currents and fields in the diamond amplifier.

We measured electron emission of the hydrogenated samples from the improved hydrogenation system in the same system as before. The original multiple-hole anode was replaced with a new anode with one smaller hole. The new anode assured that the field was more even in the emission area. The primary beam was a 10 keV DC

electron beam with typical current of about 300 nA. A pull-push HV switch circuit, with a rise and fall time of 20 ns, provided the negative high voltage pulses applied on the cathode. The HV's pulse width, amplitude and its repetition frequency (typically 1 kHz) were controlled accurately. We measured the average emission current by measuring the current of the integrated anode current. The emission spot, the same as the primary beam spot, was offset from the centre such that the leakage current from the anode hole was negligible, or only the primary electron beam, proving that emission only occurred during the HV pulses with the primary beam. Therefore, the emission duty-cycle in our test was the ratio of the HV pulse's width and the repetition period. Figure 4 shows the average gain as a function of pulse width at a field in the diamond of 0.88 MV/m, 1.76 MV/m, and 2.94 MV/m during the pulses. The maximum gain was about 140 at a high-voltage pulse-width of 200 ns under a field of 0.88 MV/m.

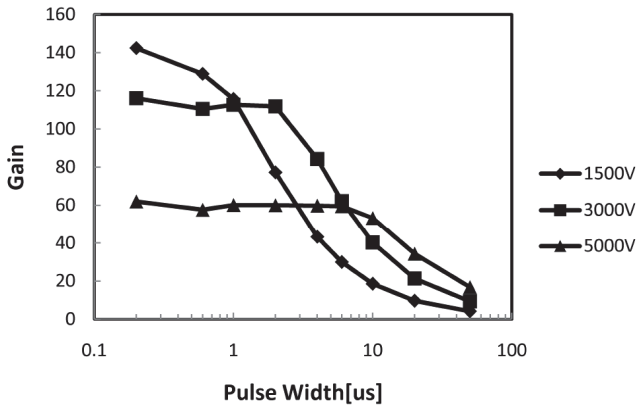


Figure 4: Average emission gain in HV pulses as a function of the pulse's width. HV amplitude of 1.5 kV, 3 kV, and 5 kV respectively corresponds to a field in diamond of 0.88 MV/m, 1.76 MV/m, and 2.94 MV/m during the pulses.

### DERIVATION OF THE TIME DEPENDENT INTERNAL FIELD

We want to extract from the measurements of the average emission current  $I_a$  as a function of applied field and pulse length the instantaneous emission probability, defined as  $P=I_e/I_i$ . In a very short high-voltage pulse width ( $\ll \mu s$ ), when the density of the surface-trapped electrons is insufficient to shield the external field, the emission probability is equal to  $P=I_a/(I_i \cdot w \cdot f)$  or equivalently  $P=G_e/G_t$ . Based on these definitions, we can write the time-dependent internal field. The internal field is the vector sum of the external field and the field induced by the density of trapped electrons. For calculating the internal field in the surface-trapped diamond amplifier, we used the capacitor model. The internal field is given by

$$E_i(t) = \frac{E_e(t)}{\epsilon_r} - \frac{\sigma(t)}{\epsilon} \quad (1)$$

Where  $E_e/\epsilon_r$  is the internal field without surface trapping,  $\epsilon_r$  is the relative permittivity of pure diamond and  $\epsilon$  is the permittivity of the diamond.  $\sigma(t)$  is the density of trapped electrons on the surface. In our emission test setup, we applied a constant high voltage pulse to the diamond's metal coating, and the anode was grounded.

The surface electron-trapping and the reduction in the internal field are described by

$$E_i(t) = \frac{E_e(t)}{\epsilon_r} - \frac{1}{\epsilon \times S} \int_0^t (1-P) \times I_p \times G_t(E_p, E_i(t)) dt$$

Where  $E_e(t)$  is the external field and the transmission gain  $G_t$  is a function of the energy of the primary electrons  $E_p$ , and the diamond's internal electric field,  $E_i$ . The time-dependence is induced by the variations in the internal electric field  $E_i(t)$  due to shielding by the trapped charge. The details of derivation are published elsewhere[4]. To solve this integral equation, we must know the amplifier's transmission gain  $G_t$  and the probability of emission  $P$ .

The transmission gain is defined as the ratio of the current of the secondary electrons reaching the emission surface to the primary-electron current[5]. We find that the gain fits rather well to an easy functional dependence which includes the primary electron's energy and the field in the diamond as follows,

$$G_t(E_p, E_i(t)) = (a[1/keV]E_p[keV] - b)(1 - e^{-c[m/M]E_i(t)[M/m]}) \quad (3)$$

where  $E_p$  is the primary electron's energy, and  $E_i(t)$  is the time-dependent internal field. The points in Figure 2 show transmission gain as a function of internal field measured for a diamond sample. In the combined best fit of Eqn. 6 to the data, yields  $a=52.5$ ,  $b=173.2$ , and  $c=4.1$ .

### EMISSION PROBABILITY

Next, we obtained the emission probability using the Schottky model applied to the Negative Electron Affinity (NEA) of the hydrogenated diamond's surface. The effective NEA model is described as a combination of positive electron-affinity and the bending of the depletion band at the surface of the semiconductor. In our measure, we found that electrons are trapped at the emission surface, and furthermore, that the trapping rate is a function of the external field. The potential surface barrier prevent electrons with energy below this barrier from escaping the diamond and the modification of this barrier by the applied field changes the number of electrons that can escape, thus leading to a measurement of the electrons' energy distribution.

We used four practically identical single-crystal, high-purity CVD diamonds [100] to fabricate four diamond amplifiers by applying a thin metal layer on one surface, and hydrogen termination of the other surface.

We carried out the experiment by measuring the emission current as a function of the pulse's length and the strength of the applied field. Figure 5 shows the  $G_e/G_t$  of four diamonds as a function of the external field where we used a very small pulse width (200ns). Under this very short pulse, and the primary current that we applied (200 nA), the change in the internal field can be neglected, and the instantaneous emission probability,  $P$ , is equal to  $G_e/G_t$ .

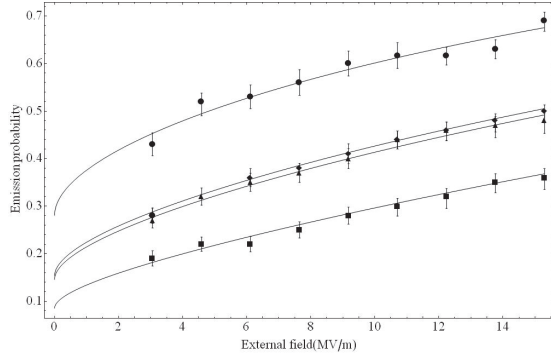


Figure 5: The dependence of emission probability  $P$  on the external field when the pulse width is 200ns. The points were measured from four different diamond samples. The four solid lines were generated by fitting to Eqn. 6, below.

We adopted the Schottky effect on the effective NEA surface to explain why emission probability depends on the external field. The external electric field and the force from image charges inside the diamond reduce the electron's potential energy. The difference between the maximum value of the potential and the vacuum level is given by

$$\phi_s = \sqrt{\frac{eE_e}{4\pi\epsilon_0} \left( \frac{\epsilon - \epsilon_0}{\epsilon + \epsilon_0} \right)} \quad (4)$$

The diamond's relative permittivity is 5.6, the Schottky potential simplifies to  $0.0318(E_e(\text{MV/m}))^{0.5}[\text{eV}]$ . The Schottky effect reduces the surface potential barrier, thus allowing the emission of electrons with a lower energy. Figure 6 shows the diamond surface's band structure. As secondary electrons reach the emission surface, some get into the potential well between the conduction band and the Schottky potential. The minimum energy of the secondary electron is the same as that of the CBM at surface. We define  $\phi_1$  as the energy difference from the CBM to the vacuum level. The  $\phi_1$  reduce in the potential  $\phi_s$  due to Schottky effect. Electrons can escape the diamond either with energies great than  $\phi_1 - \phi_s$ , or by tunnelling through the barrier.

We find that fitting the current dependence on the applied field to an expression [6] used for tunnelling does not lead to a good fit to the experimental data. On the other hand, we get a good fit making the assumption that

only electrons above the Schottky barrier escape and neglecting tunnelling altogether.

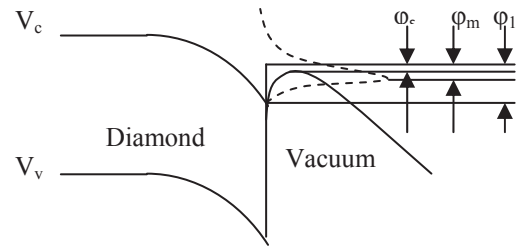


Figure 6: Energy-level diagram of diamond amplifier vacuum interface band structure. The dashed curve represents the internal distribution of the secondary electrons' energy.  $\phi_m$  is the energy difference between the mean of distribution of internal electron energy and the vacuum level.

The emission probability also is related to the energy distribution of electrons inside the diamond. The energy distribution of the electrons emitted from a surface depends strongly on the position of vacuum level and the Schottky potential, which are related to the external field.

As a first approximation, we model the distribution of secondary electrons in diamond near the emission surface (close to the end of the band bending region) with a Gaussian given by

$$f(\phi) = \frac{e^{-\frac{(\phi-m)^2}{2\sigma^2}}}{\sqrt{2\pi\sigma^2}} \quad (5)$$

where  $\sigma$  is the variance, and we chose the mean as  $m$  relative to CBM at the surface.  $\phi$  is taken as the energy above the CBM. For the electrons with energy lower than  $\phi_1 - \phi_s$ , the probability of escape is assumed negligible.

Therefore, the probability of secondary-electron emission is

$$P = 1 - \frac{1}{2} \text{Erfc}\left(\frac{\phi_m + \phi_s}{\sqrt{2}\sigma}\right) \quad (6)$$

where  $\phi_m$  is the energy difference between the mean of distribution of internal electron energy and the vacuum level. The values of  $\sigma$  and  $\phi_m$  now are found by fitting to the experimental data (Figure 5).

Since all four diamond samples were of the same thickness, crystal orientation, and purity, we assume that the internal distribution of secondary electrons is same in all of them under the same measurement conditions. However, the level of the NEA may differ among these samples, as is reflected by changes in  $\phi_m$ . The internal energy-spread,  $\sigma$ , obtained from the best fit is  $0.12 \pm 0.01\text{eV}$ , in agreement with simulation showing that  $\sigma$  is  $0.13\text{eV}$  to  $0.14\text{eV}$ [7]. For the four diamonds, the values of  $\phi_m$  obtained from the fitting are  $-0.070\text{eV}$ ,  $-0.123\text{eV}$ ,  $-0.127\text{eV}$ , and  $-0.165\text{eV}$ . The vacuum level of the different samples might vary due to several effects, such as hydrogen coverage [8], surface-carbon orientation[9], and the orientation of the C-H bond in the hydrogen-

terminated surface [10]. Eqn. 6 gives the initial emission-probability response to the external field with a certain  $\sigma$  and  $\phi_m$ , regardless of how it is determined.

The band structure calculations of Watanabe et al[11] show that for applied fields lower than 10 MV/m, the normalized energy distribution per unit energy divided by the density of states (DOS) behaves as a non-normalized Boltzmann distribution with effective temperature (Fig. 7(a) in their paper). However, their results are for electron transport in bulk diamond and do not take into account how the band bending region affects the distribution of electrons as a function of energy. We considered fitting the observed simulations data for the number of electrons per unit energy with a Boltzmann distribution times a model DOS given by  $\sqrt{E}$  but a better fit was obtained using a simple Gaussian distribution. A more detailed theoretical model is needed to obtain better understanding of the energy distribution of electrons near the emission surface that also takes into account the band bending effects.

The electron's energy spread near the emission surface is not determined by the energy of the nascent electrons; in drifting through the diamond, the electrons undergo a vast number of collisions, both elastic and inelastic. The energy spread of the electrons is the product of equilibrium between the small energy gain during their transit from the internal field, and their energy loss due to the frequent scattering they experience. For the intrinsic diamond, the energy of the conduction band above the Fermi energy is 2.775eV. We obtained that the equilibrium electron random energy is 0.04eV, and IMFP is 12nm when the internal field is 2MV/m. This calculated random energy of the electron is much smaller than the measured width  $\sigma$  of the Gaussian distribution above the conduction band obtained from the Schottky model.

## SOLVING THE INTEGRAL EQUATION

After we have established the emission probability, Eqn.2 can be solved numerically to obtain the pulse-length dependence of the emission current. We now insert the emission probability, Eqn. 6, and the transmission gain, Eqn. 3, into the integral Eqn. 2. The integral equation is solved numerically to generate the internal electric field as a function of time along the pulse length. Once this is known, average emission current and average emission gain can be calculated. Figures 7 illustrate our results.

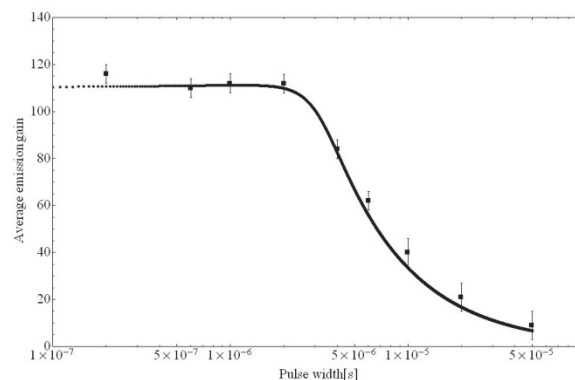


Figure 7: The results of resolving Eqn.2 are the average emission gain, and the time dependence of internal field for an applied voltage of 3000V. The solid squares are the experimental results accompanied by the estimated systematic error bars. The continuous curves are the solution of Eqn. 2.

## CONCLUSIONS

We studied the effect of hydrogenation on the NEA surface of diamond amplifiers and result in a reproducibly better performance of diamond amplifiers. We measured the emission probability of the diamond amplifier as a function of the external field and modelled the process with the resulting changes in the vacuum level due to the Schottky effect. Based on our measurement of four diamond samples with different effective NEAs, we obtained the distribution of the secondary-electrons' internal energy. We demonstrated that the average decrease in the secondary-electrons' emission-gain was a function of the pulse width, and related this to the trapping of electrons by the effective NEA surface.

## REFERENCES

- [1] X. Chang *et al.*, Phys. Rev. Lett. **105**, 164801 (2010).
- [2] E. Wang *et al.*, Physical Review Special Topics - Accelerators and Beams **14**, 61302 (2011).
- [3] G. Piantanida *et al.*, J. Appl. Phys. **89**, 8259 (2001).
- [4] E. Wang *et al.*, Physical Review Special Topics - Accelerators and Beams **14**, 111301 (2011).
- [5] X. Chang *et al.*, in Proceedings of 2007 Particle Accelerator Conference Albuquerque, NM, USA, 2007), p. 2044.
- [6] R. H. Fowler, and L. Nordheim, in *Proc. R.Soc. Lond. A May 11928*), pp. 173.
- [7] D. Dimitrov, R. Busby, and D. Mithe, in Proceedings of 2011 Particle Accelerator Conference, New York, NY, USA, WEP161, (2011).
- [8] I. L. Krainsky, and V. M. Asnin, Appl Phys Lett **72**, 2574 (1998).
- [9] J. Furthmuller, J. Hafner, and G. Kresse, Phys Rev B **53**, 7334 (1996).
- [10] Z. Zhang, M. Wensell, and J. Bernholc, Phys Rev B **51**, 5291 (1995).
- [11] T. Watanabe *et al.*, J Appl Phys **95**, 4866 (2004).